Interface solitons in locally linked two-dimensional lattices

M. D. Petrović[1], G. Gligorić[1], A. Maluckov[2], Lj. Hadžievski[1], and B. A. Malomed[3]
[1] *Vinča Institute of Nuclear Sciences, University of Belgrade, P. O. B. 522,11001 Belgrade, Serbia*
[2] *Faculty of Sciences and Mathematics, University of Niš, P. O. B. 224, 18000 Niš, Serbia*
[3] *Department of Physical Electronics, School of Electrical Engineering, Faculty of Engineering, Tel Aviv University, Tel Aviv 69978, Israel*

Existence, stability and dynamics of soliton complexes, centered at the site of a single transverse link connecting two parallel 2D (two-dimensional) lattices, are investigated. The system with the on-site cubic self-focusing nonlinearity is modeled by the pair of discrete nonlinear Schrödinger equations linearly coupled at the single site. Symmetric, antisymmetric and asymmetric complexes are constructed by means of the variational approximation (VA) and numerical methods. The VA demonstrates that the antisymmetric soliton complexes exist in the entire parameter space, while the symmetric and asymmetric modes can be found below a critical value of the coupling parameter. Numerical results confirm these predictions. The symmetric complexes are destabilized via a supercritical symmetry-breaking pitchfork bifurcation, which gives rise to stable asymmetric modes. The antisymmetric complexes are subject to oscillatory and exponentially instabilities in narrow parametric regions. In bistability areas, stable antisymmetric solitons coexist with either symmetric or asymmetric ones.

PACS numbers: 03.75.Lm; 05.45.Yv

I. INTRODUCTION

Solitons trapped at interfaces between different nonlinear media [1], [2], or pinned by defects [3–8], have been the subject of many recent studies. It has been found that the self-trapped surface modes possess novel properties in comparison with the solitons in bulk media. Among noteworthy features of these localized modes are a threshold value of the norm, above which they exist, and the coexistence of different surface modes with equal norms.

The studies of interface solitons in discrete systems have shown that spatially localized states with broken symmetries can exist [5], which may be related to the general phenomenon of the spontaneous symmetry breaking (SSB) in bimodal nonlinear symmetric settings with a linear coupling between two subsystems. For the first time, the SSB bifurcation, which destabilizes symmetric states and gives rise to asymmetric ones, was predicted in a discrete self-trapping model in Ref. [9]. This finding was followed by the prediction of the SSB in the model of dual-core nonlinear optical fibers [10], [11]. In the framework of the nonlinear Schrödinger (NLS) equation, the concept of the SSB was, as a matter of fact, first put forward in early work [12]. Related to this context is the analysis of the SSB of discrete solitons in the system of linearly coupled 1D and 2D (one- and two-dimensional) discrete nonlinear-Schrödinger (DNLS) equations [13] (the general outline of the topic of DNLS equations was given in book [14]).

The SSB was also analyzed in detail for solitons in the continual model of dual-core fibers with the cubic (Kerr) nonlinearity [15]-[17], and in related models of Bose-Einstein condensates (BEC's) loaded into a pair of parallel-coupled cigar-shaped traps [18]. In the latter context, the analysis was generalized for 2D coupled systems [19]. The SSB for gap solitons was studied too, in the model of dual-core fiber Bragg gratings [20], and later in the model of the BEC trapped in the dual-trough potential structure, combined with a longitudinal periodic potential [21]. As concerns the relation between discrete and continual systems, it is relevant to mention work [22], where exact analytical solutions were found for the SSB in the model with the nonlinear coefficient in the form of a pair of delta-functions embedded into a linear medium. In its own turn, the latter model has its own discrete counterparts, in the form of a pair of nonlinear sites embedded into a linear chain [23, 24], or side-coupled to its [25]. These models may be realized in terms of BEC and optics alike. The SSB in such settings was recently analyzed in Refs. [24] and [25], respectively.

Coming back to discrete media, the objective of the present work is to study localized modes at the interface of two 2D uniform lattices with the cubic on-site self-focusing, which are linearly linked at a single site. This link plays the role of the interface. Accordingly, the localized modes are complexes formed by two fundamental solitons in each lattice, centered at the linkage site. We focus on the symmetry of the soliton complexes, with the intention to investigate the SSB transitions in them.

This work is a natural extension of the recent study of interface modes in the system of single-site-coupled 1D nonlinear lattices [26]. Unlike the 1D situation, it would be difficult to realize such a 2D setting in optics. However, it is quite possible in BEC: one may consider two parallel pancake-shaped traps combined with a deep 2D optical lattice traversing both pancakes [27], with the local link induced by a perpendicular narrow laser beam. In fact, similar two-tier layers of nonlinear oscillators, transversely linked at sparse sites, can be realized in a number of artificially built systems.

The article is organized as follows. The model is formulated in Section 2. In the same section the existence and stability of various on-site-centered fundamental localized modes are considered in a quasi-analytical form by means of the variational approximation (VA) and Vakhitov-Kolokolov (VK) stability criterion. Numerical results for the soliton complexes are presented in Section 3, including the stability and dynamics. The numerical findings are compared to the predictions of the VA, and both the analytical and numerical results are compared to those reported in Ref. [26] for the fundamental localized modes in the 1D counterpart of the system with parallel-coupled lattices, or 'system 2', in terms of Ref. [26]). The paper is concluded by Section 4.

II. THE MODEL AND VARIATIONAL APPROXIMATION

A. The formulation

The set of the locally linked 2D uniform lattices is displayed in Fig. 1. The intra-site coupling constant in the lattices is $C > 0$, and $\varepsilon > 0$ is the strength of the transverse link. The lattice system is modeled by the following DNLS system,

$$\begin{aligned} i\frac{d\phi_{n,m}}{dt} + \frac{C}{2}(\phi_{n+1,m} + \phi_{n-1,m} + \phi_{n,m+1} + \phi_{n,m-1} - 4\phi_{n,m}) + \varepsilon\psi_{n,m}\delta_{n,0}\delta_{m,0} + \gamma\left|\phi_{n,m}\right|^2\phi_{n,m} &= 0, \\ i\frac{d\psi_{n,m}}{dt} + \frac{C}{2}(\psi_{n+1,m} + \psi_{n-1,m} + \psi_{n,m+1} + \psi_{n,m-1} - 4\psi_{n,m}) + \varepsilon\phi_{n,m}\delta_{n,0}\delta_{m,0} + \gamma\left|\psi_{n,m}\right|^2\psi_{n,m} &= 0, \end{aligned} \tag{1}$$

where $\gamma > 0$ is the coefficient of the on-site self-focusing nonlinearity, t is the time, and $\delta_{m,n}$ is the Kronecker's symbol. By means of obvious rescaling, we set $C/2 = \gamma = 1$.

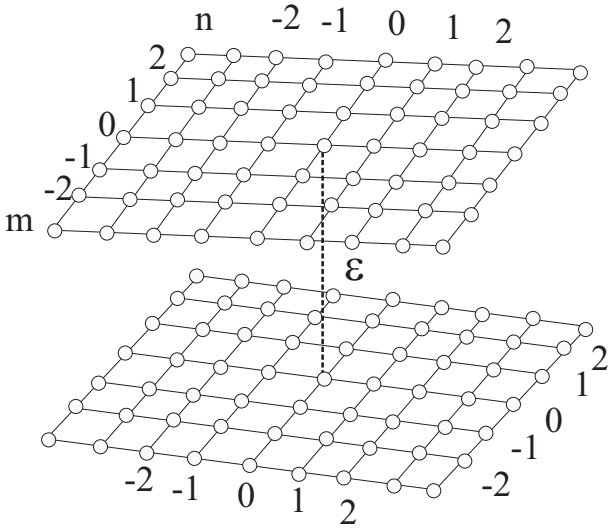

FIG. 1: (Color online) A schematic presentation of parallel 2D identical latices, linearly linked at the single site $n = m = 0$, with the coupling constant ε.

To construct soliton complexes formed around the transverse link, we look for stationary solutions, $\phi_{n,m} = u_{n,m}\exp(-i\mu t)$, $\psi_{n,m} = v_{n,m}\exp(-i\mu t)$, where $u_{n,m}, v_{n,m}$ and μ are real lattice fields and the propagation constant, respectively. The corresponding stationary equations following from Eqs. (1) are

$$\begin{aligned} \mu u_{n,m} + (u_{n+1,m} + u_{n-1,m} + u_{n,m+1} + u_{n,m-1} - 4u_{n,m}) + \varepsilon v_{n,m}\delta_{n,0}\delta_{m,0} + \left|u_{n,m}\right|^2 u_{n,m} &= 0, \\ \mu v_{n,m} + (v_{n+1,m} + v_{n-1,m} + v_{n,m+1} + v_{n,m-1} - 4v_{n,m}) + \varepsilon u_{n,m}\delta_{n,0}\delta_{m,0} + \left|v_{n,m}\right|^2 v_{n,m} &= 0. \end{aligned} \tag{2}$$

Equations (2) can be derived from the Lagrangian,

$$L = L_u + L_v + 2\varepsilon u_{0,0}v_{0,0}, \tag{3}$$

$$L_u \equiv \sum_{n=-\infty}^{+\infty}\sum_{m=-\infty}^{+\infty}\left((\mu-4)u_{n,m}^2 + \frac{1}{2}u_{n,m}^4 + 2u_{n,m}(u_{n+1,m} + u_{n,m+1})\right),$$

$$L_v \equiv \sum_{n=-\infty}^{+\infty} \sum_{m=-\infty}^{+\infty} \left((\mu - 4) v_{n,m}^2 + \frac{1}{2} v_{n,m}^4 + 2 v_{n,m} (v_{n+1,m} + v_{n,m+1}) \right), \tag{4}$$

where L_u and L_v are the intrinsic Lagrangians of the uncoupled lattices, and the last term in Eq. (3) accounts for the coupling between them.

B. The variational approximation

The variational method follows the route described in Ref. [13]. We adopt a natural ansatz, which was first applied to discrete lattices in Ref. [28]:

$$\{u_{m,n}, v_{n,m}\} = \{A, B\} \exp(-a|n|) \exp(-a|m|), \tag{5}$$

where A and B (but not a, see below) are treated as variational parameters. This form of the trial function admits different amplitudes, $A \neq B$, of the solutions in the coupled lattices, but postulates equal widths in both of them, a^{-1}. In this context, the SSB is signaled by the emergence of asymmetric solutions, with $A^2 \neq B^2$ [13, 26].

The inverse width a of the localized trial solution is found independently from the linearization of Eqs. (2), which is valid in the soliton's tails (at $|m|, |n| \to \infty$),

$$a = -\ln \left((4 - \mu)/4 - \sqrt{(4 - \mu)^2/16 - 1} \right), \tag{6}$$

provided that the propagation constant is negative, $\mu < 0$ (otherwise, the solution cannot be localized). Relation (6) may also be cast in another form, that will be used below:

$$s \equiv e^{-a} = \frac{4 - \mu}{4} - \sqrt{\frac{(4 - \mu)^2}{16} - 1}, \ \mu = 4 - 2(s + s^{-1}). \tag{7}$$

The substitution of ansatz (5) into Eqs. (3) and (4) yields the corresponding effective Lagrangian with two variational parameters A and B, where Eq. (7) is used to eliminate μ in favor of s:

$$L_{\rm eff} = (L_u)_{\rm eff} + (L_v)_{\rm eff} + 2\varepsilon AB, \tag{8}$$

$$\begin{aligned} (L_u)_{\rm eff} &= -2A^2 \frac{1 + s^2}{s} + \frac{1}{2} A^4 \frac{(1 + s^4)^2}{(1 - s^4)^2}, \\ (L_v)_{\rm eff} &= -2B^2 \frac{1 + s^2}{s} + \frac{1}{2} B^4 \frac{(1 + s^4)^2}{(1 - s^4)^2}. \end{aligned} \tag{9}$$

The Euler-Lagrange equations for amplitudes A and B are $(\partial/\partial A)(L_u)_{\rm eff} + 2\varepsilon B = 0, (\partial/\partial B)(L_v)_{\rm eff} + 2\varepsilon A = 0$, or, in the explicit form,

$$\begin{aligned} -2\frac{1 + s^2}{s} A + \frac{(1 + s^4)^2}{(1 - s^4)^2} A^3 + \varepsilon B &= 0 \\ -2\frac{1 + s^2}{s} B + \frac{(1 + s^4)^2}{(1 - s^4)^2} B^3 + \varepsilon A &= 0. \end{aligned} \tag{10}$$

These equations allow us to predict the existence of three different types of the complexes formed by the fundamental localized modes centered at the linkage site: symmetric and antisymmetric ones, with $A = B$ and $A = -B$, respectively, and asymmetric modes with $A^2 \neq B^2$.

1. *Existence regions for the interface soliton complexes*

The solution for the symmetric soliton complexes is easily obtained from Eqs. (10):

$$A^2 = \frac{(1 - s^4)^2}{(1 + s^4)^2} \left[\frac{2}{s} (1 + s^2) - \varepsilon \right]. \tag{11}$$

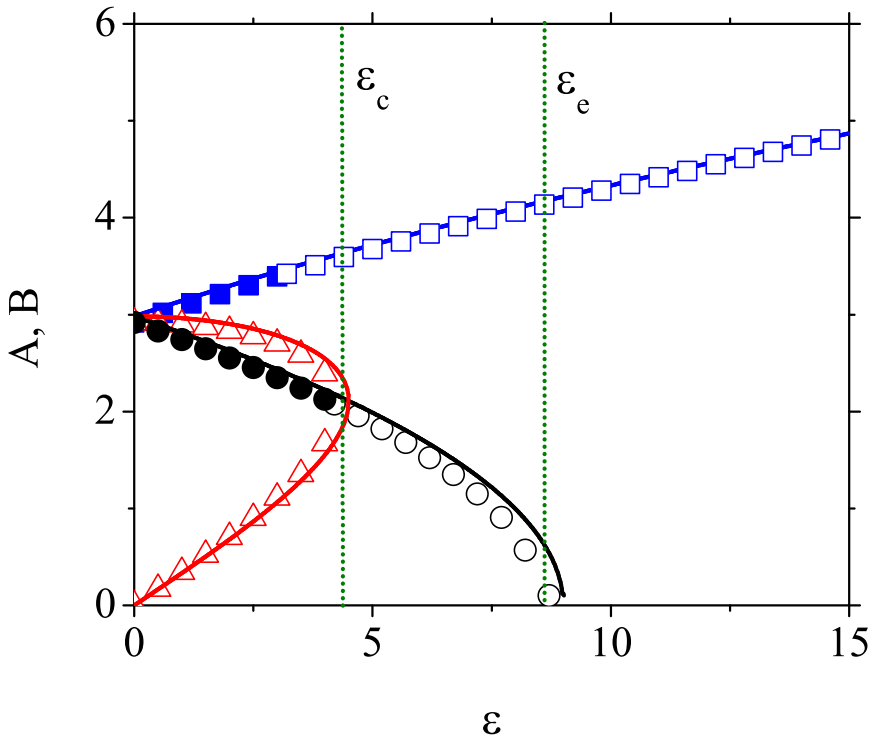

FIG. 2: (Color online) Amplitudes A and B of asymmetric, symmetric, and antisymmetric solitons (red, black, and blue colors, respectively), as predicted by the variational approximation (lines) and obtained in the numerical form (triangles, circles, and squares pertain to the asymmetric, symmetric, and antisymmetric modes, respectively) vs. the inter-lattice linkage strength ε. The propagation constant is fixed to $\mu = -5$. The dotted green vertical lines denote the numerically found critical values of ε limiting the existence regions of the asymmetric (ε_c) and symmetric (ε_e) solitons. Filled and empty symbols correspond to unstable and stable solitons, respectively, as concluded from the numerical investigation.

As follows from Eq. (11), the existence domain of the symmetric solutions is $\varepsilon < \varepsilon_e \equiv 2(1+s^2)/s$. For $\mu = -5$, solution branches of all the types, produced by the VA along with their numerical counterparts, are shown in Fig. 2, and the respective existence regions, including the one given by curve $\varepsilon_e(\mu)$, is displayed in Fig. 3. The procedure for obtaining numerical results is described below.

The amplitudes and existence range of the asymmetric solution complexes, with $A^2 \neq B^2$, can be calculated by adding and subtracting Eqs. (10). After a straightforward procedure, the following expressions for the amplitudes are obtained:

$$\begin{aligned} A &= \pm \frac{(1-s^4)}{(1+s^4)\sqrt{s}} \sqrt{1+s^2+\sqrt{(1+s^2)^2-\varepsilon^2 s^2}}, \\ B &= \frac{(1-s^4)^2}{(1+s^4)^2} \frac{\varepsilon}{A}. \end{aligned} \tag{12}$$

This soliton mode exists at $\varepsilon < \varepsilon_c \equiv (1+s^2)/s$, where ε_c is the bifurcation value. The existence of the asymmetric mode may be naturally expected when the linkage constant (ε) is not too large [13], [15]-[19]. Indeed, the ultimate asymmetric solution, with $A \neq 0$ and $B = 0$, is obviously possible in the limit of $\varepsilon = 0$, which corresponds for the decoupled lattices. It is also natural that, with the decrease of ε, the symmetry-breaking bifurcation should occur at some $\varepsilon = \varepsilon_c$, where the two asymmetric branches emerge from the symmetric one, see Fig. 2. However, the stability of the related solutions cannot be predicted solely by the VA.

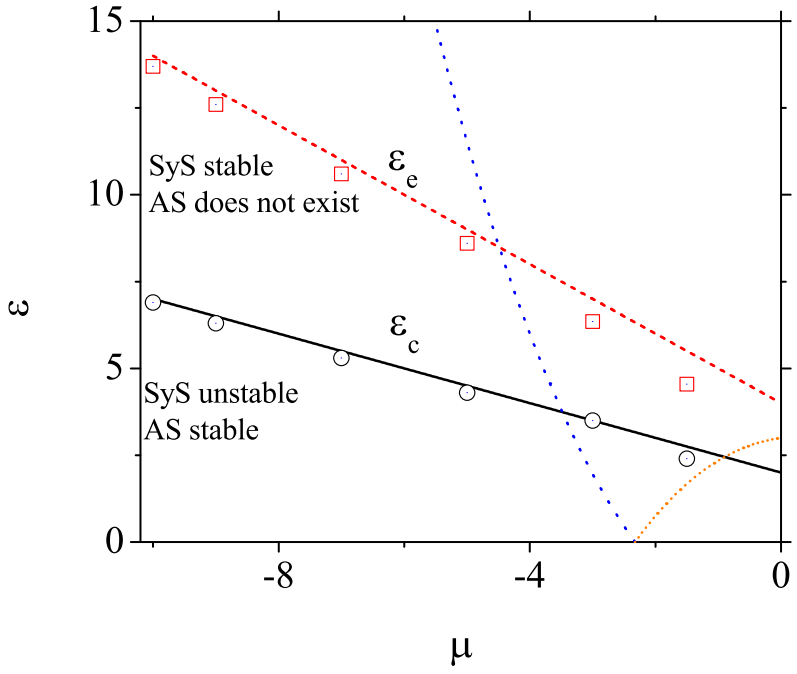

FIG. 3: (Color online) The existence and stability diagrams for the fundamental symmetric (SyS), asymmetric (AS) and antisymmetric (AnS) solitons. The variational results are presented by curves, and numerical findings—by symbols in the parameter space (ε, μ). Black circles and the corresponding line mark the boundary of the AS existence region. Red squares and the dashed line denote the existence boundary for the SyS modes. The numerical calculations show that the symmetry-breaking bifurcation takes place along the curve $\varepsilon_c(\mu)$. The AnS mode exists in the entire parameter plane. According to the Vakhitov-Kolokolov criterion, the AS may be stable in the whole existence region, the SyS may be stable above the orange dashed line, and AnS—to the left from the blue dotted line. The stability type of the SyS and AS modes, indicated in the figure, was established by means of numerical computations.

For antisymmetric soliton complexes, the amplitude is obtained from Eq. (10) by setting $A = -B$, which yields

$$A^2 = \frac{(1-s^4)^2}{(1+s^4)^2}\left[\frac{2}{s}(1+s^2)+\varepsilon\right], \tag{13}$$

cf. Eq. (11) for the symmetric modes. Relation (13) is plotted versus ε for fixed $\mu = -5$ by the blue (upper) curve in Fig. 2. As follows from this relation, the VA predicts the existence of the antisymmetric solitons in the entire parameter space, on the contrary to the limited existence regions predicted for the symmetric and asymmetric modes.

2. *Stability of the soliton complexes*

The stability of the discrete solitons predicted by the VA can be estimated by dint of the VK criterion, $dP/d\mu > 0$, where $P \equiv \sum_{n=-\infty}^{n=+\infty}\sum_{m=-\infty}^{m=+\infty}(u_{n,m}^2 + v_{n,m}^2)$ is the total norm (power) of the soliton complex [29]. The norm corresponding to the ansatz (5) is

$$P = (A^2+B^2)\left(\frac{1+s^2}{1-s^2}\right)^2. \tag{14}$$

For the symmetric solution with $A = B$, Eqs. (11) and (14) yield

$$P = 2\frac{(1+s^2)^4}{(1+s^4)^2}\left[\frac{2}{s}(1+s^2)-\varepsilon\right]. \tag{15}$$

This expression satisfies condition $\partial P/\partial s < 0$, which is tantamount to the VK criterion, in the region of

$$\varepsilon > \frac{2(1+s^2)}{s} - \frac{(1+s^2)(1+s^4)}{4s^3}. \tag{16}$$

This region is displayed in Fig. (3) as the area above the dashed orange curve (in the right bottom corner of the figure). Thus, according to the VK criterion, the stable symmetric branch may exist in the large part of the parameter plane, except for the small region below the dashed orange curve, which corresponds to the weak inter-lattice linkage and wide solitons.

For the asymmetric solutions, the substitution of Eq. (12) into Eq. (14) produces a simple expression for the total norm, which does not depend on ε:

$$P = 2\frac{(1+s^2)^5}{s(1+s^4)^2}. \tag{17}$$

It also satisfies the VK criterion in the entire region of the existence of the asymmetric mode.

For the antisymmetric modes with $A = -B$, the use of Eq. (13) gives

$$P = 2\frac{(1+s^2)^4}{(1+s^4)^2}\left[\frac{2}{s}(1+s^2) + \varepsilon\right]. \tag{18}$$

In this case, condition $dP/ds < 0$ is satisfied at

$$\varepsilon < \frac{(1+s^2)(1+s^4)}{4s^3} - \frac{2(1+s^2)}{s}. \tag{19}$$

The region defined by Eq. (19) is shown in Fig. (3) as the area to the left from the blue dotted curve (the one which cuts the entire plane).

However, the VK criterion offers only the necessary condition for the soliton stability. To identify regions of full stability of the soliton complexes, the VK criterion should be combined with the spectral condition, which requires the existence of only pure imaginary eigenvalues in the linearization of Eqs. (1) with respect to small perturbations around the stationary soliton solutions. The spectral analysis is performed numerically in the next section. In fact, the results demonstrate that, unlike the prediction of the shape of the soliton modes by means of the VA, the stability prediction based on the formal application of the VA criterion is not accurate.

III. NUMERICAL RESULTS

The predictions of the VA were verified by numerically solving stationary equations (2). The numerical algorithm is based on the modified Powell minimization method [30]. The initial guess to construct soliton complexes centered at the linkage site of the 2D lattices (Fig. 1) was taken as $u_0 = v_0 = A > 0$ for symmetric solutions, $u_0 = A > 0$, $v_0 = B \neq A > 0$ for asymmetric ones, and $u_0 = A > 0$, $v_0 = -A$ for solutions of the antisymmetric type, with the VA-predicted values of A and B. At other sites, the amplitudes of the initial guess are set to be zero.

A. Stationary soliton modes

The stability of the stationary modes was investigated through the calculation of eigenvalues (EVs) of small perturbations around the stationary solutions, which were computed following the lines of Refs. [26, 30, 31]. The obtained results were further verified in direct numerical simulations of Eqs. (1), using the sixth-order Runge-Kutta algorithm, as in Refs. [26, 30]. The simulations were carried out for stationary soliton complexes to which initial perturbations were added.

Typical shapes of symmetric, asymmetric and antisymmetric soliton complexes found in the numerical form are displayed in Fig. 4. The respective dependencies of the amplitudes A and B on ε were displayed above, for all the soliton branches, alongside their VA-predicted counterparts, in Figs. 2 and 3. The numerical results show that the symmetric and asymmetric complexes exist in bounded regions of the parameter space, see Fig. 3. The results predicted by means of the VA are in good agreement with their numerical counterparts for all the types of the soliton complexes. The comparison of the variational and numerical dependencies of the solitons' amplitudes on ε, for fixed $s \approx 0.23$, which corresponds to $\mu = -5$, can be seen in Fig. 2. The difference between the analytical and numerical

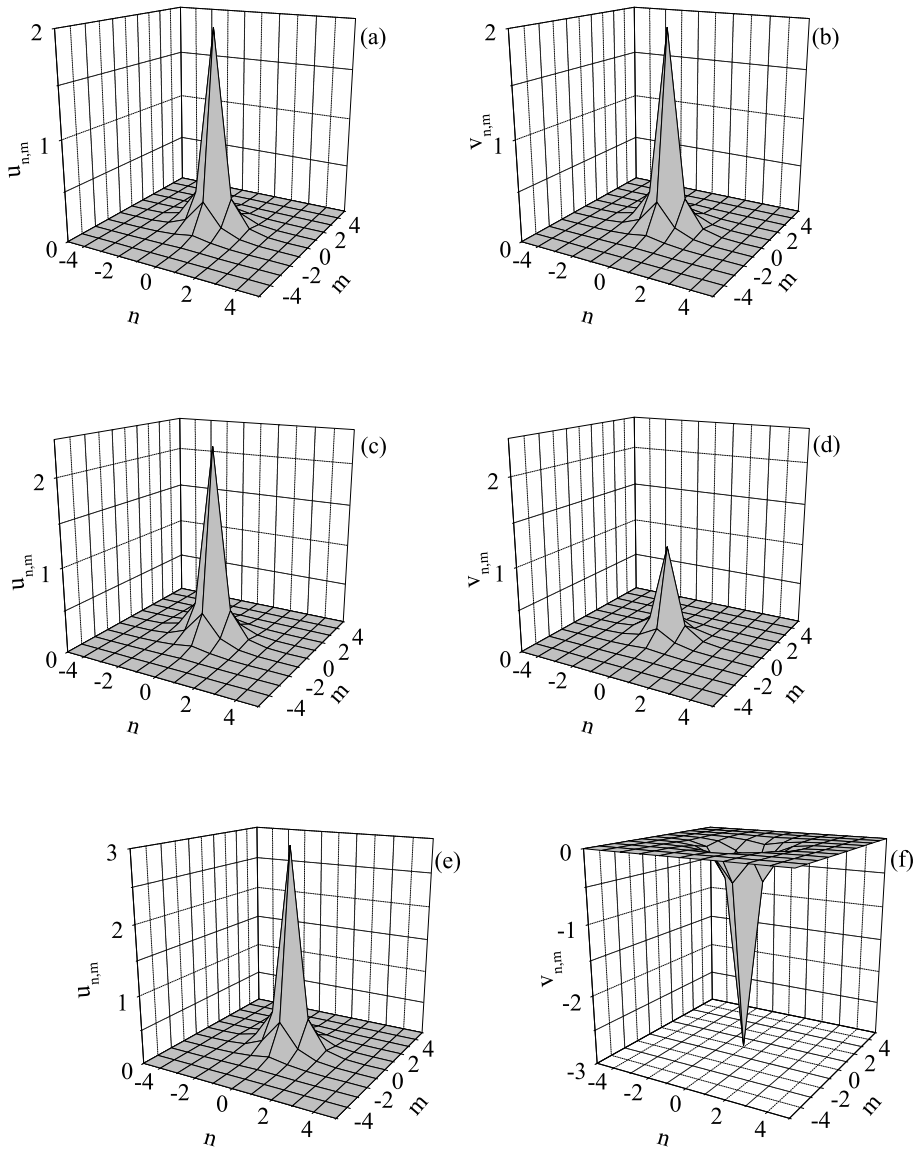

FIG. 4: Typical shapes of the soliton complexes of different types: symmetric in (a) and (b), asymmetric in (c) and (d), and antisymmetric in (e) and (f). The parameters are $\mu = -3$, $\varepsilon = 2.5$, the corresponding norms for complexes being $P_{\rm symm} = 8.63$, $P_{\rm asymm} = 7.11$, and $P_{\rm antisymm} = 19.91$.

results is negligible for small ε, and slightly grows with ε. In particular, the existence border of the symmetric complexes predicted by the VA is $\varepsilon_e \equiv 9$, while its numerical counterpart is $\varepsilon_e \equiv 8.63$.

Finally, it is easy to check that both the variational and numerical results demonstrate that the SSB pitchfork bifurcation observed in Fig. 2 is of the *supercritical* type, similarly to that reported in Ref. [26] for the 1D counterpart of the present system (in contrast with the *subcritical* bifurcation demonstrated by the system of 1D and 2D parallel chains with the uniform linear coupling acting at each site [13]).

B. The stability analysis

The linear-stability analysis demonstrates that the symmetric complexes emerge as stable solutions at $\varepsilon = \varepsilon_e$, and, as expected, they change the stability at the bifurcation point, $\varepsilon = \varepsilon_c$, where the asymmetric solution branches appear

(see Figs. 2 and 3). Unstable symmetric solutions are characterized by the pure real EV pairs, see Fig. 5(a). For the parameter set used in Fig. 5(a), the isolated discrete solitons existing in the uncoupled lattices at $\varepsilon = 0$ are stable [30, 32]. The introduction of the linkage between the lattices changes the stability of the symmetric complex formed by such solitons. The results *do not* confirm the prediction, based on the VK criterion, that the symmetric complexes change the stability at the value of the ε given by Eq. (16), which corresponds to the orange dashed curve in Fig. 3. The instantaneous destabilization of the symmetric bound states with the increase of ε from zero [see Fig. 7(a)] is simply explained by the fact that symmetric complexes are always unstable against the SSB in dual-core systems with a small linear-coupling constant [17].

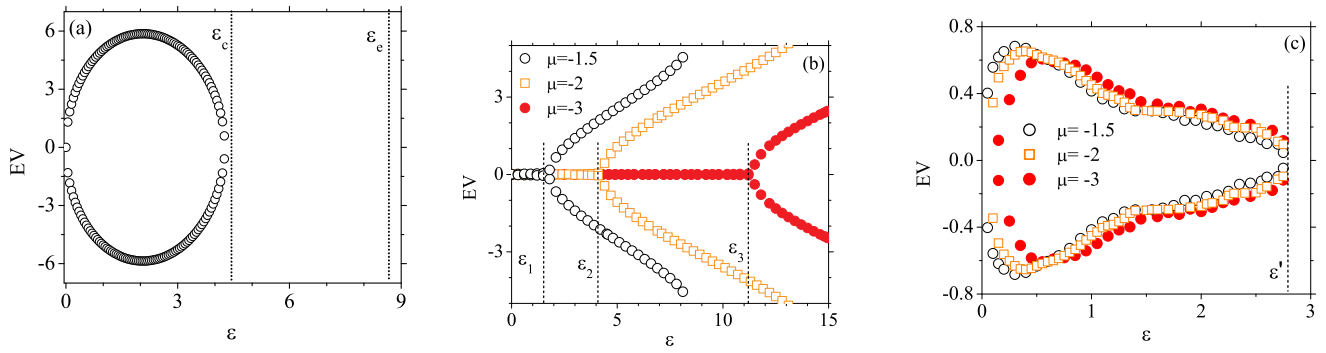

FIG. 5: (Color online) (a) Pure real eigenvalues (EVs) vs. ε for symmetric solitons with $\mu = -5$. Dotted lines denote the bifurcation value ε_c and the existence threshold ε_e for the symmetric solitons. Pure real EVs, and the real part of complex EVs, are shown vs. ε in panels (b) and (c), respectively, for antisymmetric solitons. Black (empty circles), orange (squares), and red (filled circles) symbols correspond, respectively, to fixed $\mu = -1.5, -2$, and -3. Dotted lines marked by $\varepsilon_{1,2,3}$ in plot (b), and by ε' in plot (c) are boundaries of regions where the pure real EVs (b), or real parts of the complex EVs (c), take significant values, Re(EV) > 0.001.

Direct simulations confirm the stability of the SyS complexes in the interval of $\varepsilon_c < \varepsilon < \varepsilon_e$. On the other hand, simulations of the evolution of unstable symmetric modes demonstrate that, under the action of small perturbations, these unstable modes (at $\varepsilon < \varepsilon_c$) evolve into asymmetric breathing complexes, which consist of two oscillating localized components, that exchange energy in the course of the evolution. This behavior is illustrated in Fig. 6, where the evolution of the unstable SyS mode into the AS complex is shown by plotting the amplitudes of the component solitons versus time.

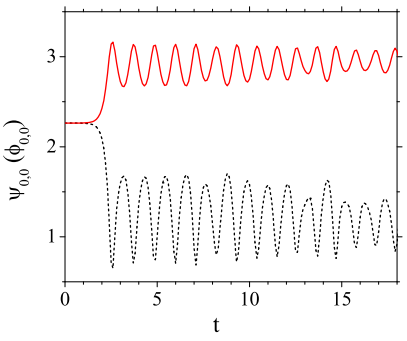

FIG. 6: The evolution of the amplitudes of the unstable SyS mode with $\mu = -5$, $\varepsilon = 3.4$ into the corresponding stable AS complex. The amplitudes of the components of the latter complex are represented by different lines.

Two mutually symmetric branches of asymmetric solutions, which are created by the destabilization of the symmetric branch, see Eq. (12), turn out to be *stable*, according to the linear-stability analysis, which yields for them EV spectra with the zero real part. Direct simulations corroborate that slightly perturbed asymmetric complexes are robust modes, see Fig. 7.

The purely real EV pairs which are numerically calculated for the antisymmetric modes become significant above

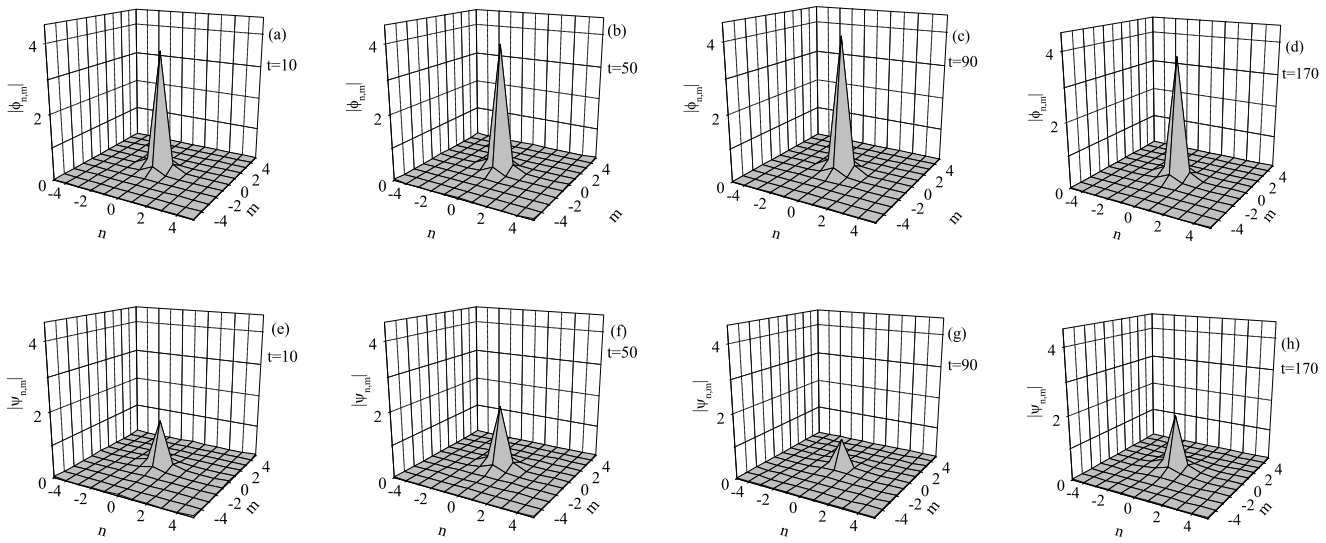

FIG. 7: The oscillatory evolution of a perturbed asymmetric complex with $P = 12.02$, $\varepsilon = 5$, and $\mu = -8$. The relative strength of small perturbation with respect to the solution amplitude is 0.01. Profiles of the two components are shown, in the top and bottom rows.

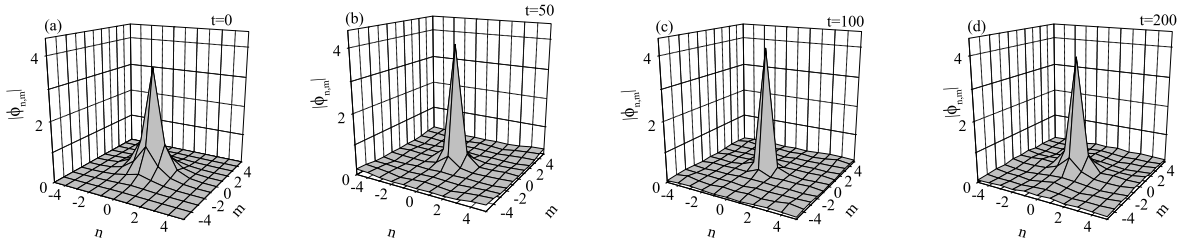

FIG. 8: The time snapshots illustrating the evolution of the AnS complex with $\mu = -1.5$, $\varepsilon = 7.2$, and $P = 33.48$. Four plots represent the amplitude profiles of the component solitons, $|\phi_{m,n}| = |\psi_{m,n}|$, at $t = 0, 50, 100$, and 200. The components are strongly pinned, with the amplitudes at the interface sites slightly oscillating around value 3.8.

some threshold values of ε, which depend on μ. The threshold values, $\varepsilon_{1,2,3}$ for $\mu = -1.5, -2, -3$, are shown in Fig. 5(b). On the other hand, the antisymmetric modes give rise to the complex EVs at $\varepsilon < \varepsilon'$ and arbitrary μ, as shown in Fig. 5(c). Therefore, at large values of the coupling constant, $\varepsilon > \varepsilon_{1,2,3}$, the instability is determined by the purely real EVs, but in the region of $\varepsilon < min(\varepsilon', \varepsilon_{1,2,3})$ the real part of the complex EV dominates the instability**.** Actually, the numerical results for the (in)stability of the antisymmetric complexes do not corroborate the analytical prediction presented by Eq. (19).

The dynamics of the antisymmetric complexes with positive real parts of the EVs is not significantly affected by small perturbations, except in the area with very small ε, where the AnS, SyS and AS with close values of the power coexist, see Fig. 3 for $\varepsilon \ll \varepsilon_c$. In the latter case, the AnS complexes follow the same scenario as the unstable SyS complexes, i.e., the unstable AnS evolves into a breathing AS complex. The reason for the robustness of other antisymmetric modes is the fact that the corresponding branch features large amplitudes of the solitons, leading to their strong trapping at the central lattice sites. Therefore, the actual instability (escape of the discrete wave fields) is suppressed by the strong the Peierls-Nabarro potential barrier [33]. Accordingly, due to the weak effective coupling between the central site and the adjacent ones, the introduction of small perturbations can excite internal oscillations but does not destroy the localization of the mode, and the emerging breather (which keeps the antisymmetric structure, as concerns the relation between its components) remains a strongly trapped state. This is the case in **almost** the whole existence region of the antisymmetric solitons. The dynamics of exponentially unstable antisymmetric complexes (actually, with large pure real EVs) is illustrated in Fig. 8 for $\mu = -1.5$ and $\varepsilon = 7.2$, with norm $P = 33.48$. Keeping the antisymmetric structure, as said above, the two components feature identical amplitude profiles, $|\psi_{n,m}| = |\phi_{n,m}|$.

Both of them shrink into more pinned modes that radiate away a small part of their norm (energy), which forms a small but finite oscillating background, while the central peak remains robust.

The instability of the antisymmetric modes in the case of very small pure real EVs develops very slowly, in the presence of small perturbations, following the same scenario. In Fig. 9, the evolution of a typical antisymmetric complex subject to the oscillatory unstable is shown. The part of the initial energy lost into background is smaller then in the previous case, and the central peak slightly oscillates in time.

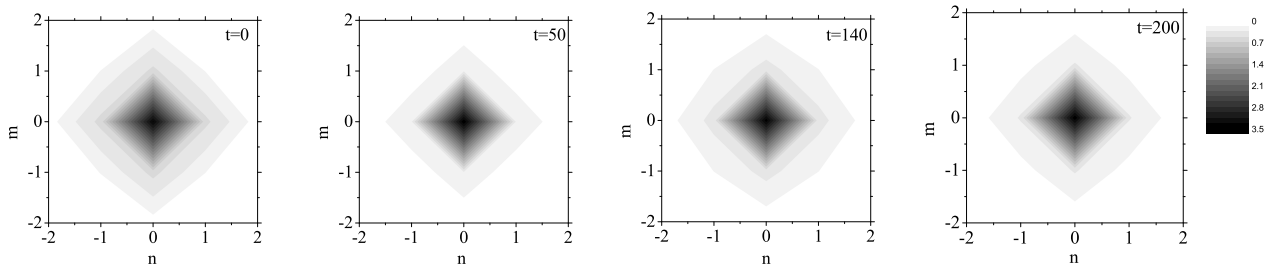

FIG. 9: The evolution of a perturbed antisymmetric mode which is unstable against oscillatory perturbations, with $\mu = -3$, $\varepsilon = 1.5$, and $P = 17.64$. The component solitons are strongly pinned, and their amplitudes slightly oscillate, similar to the case displayed in Fig. 8.

Returning to the global existence diagrams, it is worth to note that two bistability areas can be identified in them: the domain of the coexistence of stable symmetric and quasi-stable antisymmetric solitons (the quasi-stability pertains to very small growth rates mentioned above), or the one featuring the simultaneous stability of asymmetric and antisymmetric modes (at very small ε), on the opposite side on the SSB bifurcation. This result is in accordance with similar findings reported in other linearly-coupled two-component systems with the self-focusing nonlinearity [18, 19, 26].

It is also relevant to compare properties of the soliton complexes in the present two-component 2D lattice system, and on-site solitons in the uniform 2D lattice described by the single DNLS equation, which corresponds to Eqs. (2) with $\varepsilon = 0$ [30, 32]. Along the line of $\varepsilon = 0$ in Figs. 2, 3 and 5, which correspond to $\mu = -5$, one finds a stable symmetric complex, a stable asymmetric mode (with one zero component), and stable antisymmetric complexes. In terms of the uniform 2D lattice, the symmetric complex is formed of two identical on-site-centered discrete solitons, which are stable in the usual DNLS lattice [30, 32] [see, e.g., Fig. 5(a) in Ref. [30]]. As mentioned above, the introduction of the inter-lattice linkage ($\varepsilon > 0$) leads to the onset of the exponential instability in the complex formed by two identical fundamental on-site solitons. The symmetric complex recovers its stability at $\varepsilon \geq \varepsilon_c$. Therefore, one can associate two bifurcation points with values $\varepsilon = 0$ and $\varepsilon = \varepsilon_c$. The latter one was actually identified above as the supercritical pitchfork bifurcation at which the stable asymmetric branches disappear and the symmetric one is re-stabilized.

IV. CONCLUSION

In this work, we have introduced the 2D double-lattice nonlinear system, linked in the transverse direction at a single site. The system can be realized in terms of BEC, and may actually occur in a range of artificially built discrete nonlinear media. The on-site nonlinearity was considered to be self-focusing (the self-defocusing can be easily transformed the same system by means of the staggering transformation [14]). We have used the VA (variational approximation) and numerical methods to find the regions of existence, in the parameter plane of (μ, ε) (the propagation constant and the strength of the linkage between the lattices), of the localized symmetric, asymmetric and antisymmetric soliton complexes pinned to the linkage site. It was shown, by means of both approaches, that the existence regions of the symmetric and asymmetric complexes are bounded. The SSB (spontaneously symmetry-breaking) pitchfork bifurcation of the supercritical part has been found, which destabilizes the symmetric complexes and simultaneously creates stable asymmetric ones. The stability of the antisymmetric complexes changes twice. Areas of the bistability between the antisymmetric modes and either symmetric or asymmetric ones have been found too. Direct simulations demonstrate that unstable symmetric modes relax into the breathing asymmetric complexes, while the antisymmetric solitons with large amplitudes are robust against perturbations, transforming into strongly pinned breathers, which keep the antisymmetric structure.

This work also suggests a possibility to create and investigate vortex complexes in 2D parallel-coupled lattice systems, which will be reported elsewhere.

Acknowledgments

M. D. P., G. G., A. M., and Lj. H. acknowledge support from the Ministry of Education and Science, Serbia (Project III45010).

[1] K. G. Makris, S. Suntsov, D. N. Christodoulides, G. I. Stegeman, and A. Hache, Opt. Lett. **30**, 2466 (2005); M. I. Molina, R. A. Vicencio, and Y. S. Kivshar, *ibid.* **31**, 1693 (2006); Y. V. Kartashov and L. Torner, *ibid.* **31**, 2172 (2006); K. G. Makris, J. Hudock, D. N. Christodoulides, G. I. Stegeman, O. Manela, and M. Segev, *ibid.* **31**, 2774 (2006); Y. V. Kartashov, A. A. Egorov, V. A. Vysloukh, and L. Torner, Opt. Exp. **14**, 4049 (2006); D. Mihalache, D. Mazilu, F. Lederer, and Y. S. Kivshar, Opt. Exp. **15**, 589 (2007); Y.-J. He and B. A. Malomed, in book [14], p. 259.

[2] S. Suntsov, K. G. Makris, D. N. Christodoulides, G. I. Stegeman, A. Hache, R. Morandotti, H. Yang, G. Salamo, and M. Sorel, Phys. Rev. Lett. **96**, 063901 (2006); E. Smirnov , M. Stepić, C. E. Ruter, D. Kip, V. Shandarov, Opt. Lett. **15**, 2338 (2006); G. A. Siviloglou, K. G. Makris, R. Iwanow, R. Schiek, D. N. Christodoulides, G. I. Stegeman, Y. Min, and W. Sohler, Opt. Exp. **14**, 5508 (2006); X. S. Wang, A. Bezryadina, Z. G. Chen, K. G. Makris, D. N. Christodoulides, and G. I. Stegeman, Phys. Rev. Lett. **98,** 123903 (2007); A. Szameit, Y. V. Kartashov, F. Dreisow, T. Pertsch, S. Nolte, A. Tünnermann, and L. Torner, *ibid.* **98**, 173903 (2007).

[3] Yu. S. Kivshar, F. Zhang, and S. Takeno, Physica D **113**, 248 (1998).

[4] X. D. Cao and B. A. Malomed, , Phys. Lett. A **206**, 177 (1995); W. Królikowski and Y. S. Kivshar, J. Opt. Soc. Am. B **13**, 876 (1996); R. H. Goodman, R. E. Slusher, and M. I. Weinstein, *ibid.* **19**, 1635 (2002); W. C. K. Mak, B. A. Malomed, and P. L. Chu, *ibid.* **20**, 725 (2003); F. Palmero, R. Carretero-González, J. Cuevas, P. G. Kevrekidis, and W. Królikowski, *ibid.* E **77**, 036614 (2008).

[5] Yu. S. Kivshar and M. I. Molina, Wave Motion **45**, 59 (2007); M. I. Molina, and Yu. S. Kivshar, Opt. Lett. **33**, 917 (2008).

[6] U. Peschel, R. Morandotti, J. S. Aitchison, H. S. Eisenberg, and Y. Silberberg, Appl. Phys. Lett. **75**, 1348 (1999); R. Morandotti, H. S. Eisenberg, D. Mandelik, Y. Silberberg, D. Modotto, M. Sorel, C. R. Stanley, and J. S. Aitchison, Opt. Lett. **28**, 834 (2003); F. Fedele, J. K. Yang, and Z. G. Chen, *ibid.* **30**, 1506 (2005); I. Makasyuk, Z. G. Chen, and J. K. Yang, Phys. Rev. Lett. **96**, 223903 (2006); T. Schwartz, G. Bartal, S. Fishman, and M. Segev, Nature **446**, 52 (2007).

[7] R. Morandotti, H. S. Eisenberg, D. Mandelik, Y. Silberberg, D. Modotto, M. Sorel, C. R. Stanley, and J. S. Aitchison, Opt. Lett. **28**, 834 (2003).

[8] V. A. Brazhnyi and B. A. Malomed, Phys. Rev. E **83**, 016604 (2011).

[9] J. C. Eilbeck, P. S. Lomdahl, and A. C. Scott, Physica D **16**, 318 (1985).

[10] E. M. Wright, G. I. Stegeman, and S. Wabnitz, Phys. Rev. A **40**, 4455 (1989).

[11] A. W. Snyder, D. J. Mitchell, L. Poladian, D. R. Rowland, and Y. Chen, J. Opt. Soc. Am. B **8**, 2102 (1991).

[12] E. B. Davies, Comm. Math. Phys. **64**, 191 (1979).

[13] G. Herring, P. G. Kevrekidis, B. A. Malomed, R. Carretero-González, and D. J. Frantzeskakis, Physical Review E **76**, 066606 (2007).

[14] P. G. Kevrekidis, editor, *The Discrete Nonlinear Schrödinger Equation: Mathematical Analysis, Numerical Computations, and Physical Perspectives* (Springer: Berlin and Heidelberg, 2009).

[15] N. Akhmediev, and A. Ankiewicz, Phys. Rev. Lett. **70**, 2395 (1993); P. L. Chu, B. A. Malomed, and G. D. Peng,J. Opt. Soc. A B **10**, 1379 (1993); J. M. Soto-Crespo, and N. Akhmediev, Phys. Rev. E **48**, 4710 (1993).

[16] B. A. Malomed, I. Skinner, P. L. Chu, and G. D. Peng, Phys. Rev. E **53**, 4084 (1996).

[17] B. A. Malomed, in: *Progress in Optics* **43**, 71 (E. Wolf, editor: North Holland, Amsterdam, 2002).

[18] A. Gubeskys, and B. A. Malomed, Phys. Rev. A **75**, 063602 (2007); M. Matuszewski, B. A. Malomed, and M. Trippenbach, *ibid.* A **75**, 063621 (2007).

[19] A. Gubeskys and B. A. Malomed, Phys. Rev. A **76**, 043623 (2007).

[20] W. C. K. Mak, B. A. Malomed, and P. L. Chu,J. Opt. Soc. Am. B **15**, 1685 (1998); Phys. Rev. E **69**, 066610 (2004).

[21] M. Trippenbach, E. Infeld, J. Gocalek, M. Matuszewski, M. Oberthaler, and B. A. Malomed, Physical Review A **78**, 013603 (2008).

[22] T. Mayteevarunyoo, B. A. Malomed, and G. Dong, Phys. Rev. A **78**, 053601 (2008).

[23] M. I. Molina and G. Tsironis, Phys. Rev. B **47**, 15330 (1993); B. C. Gupta and K. Kundu, *ibid.* **55**, 894 (1997); **55**, 11033 (1997).

[24] V. A. Brazhnyi and B. A. Malomed, Phys. Rev. A **83**, 053844 (2011).

[25] E. Bulgakov, K. Pichugin, and A. Sadreev, Phys. Rev. B **83,** 045109 (2011).

[26] Lj. Hadžievski, G. Gligorić, A. Maluckov, and B. A. Malomed Phys. Rev. A **82**, 033806 (2010).

[27] I. Bloch, J. Dalibard, and W. Zwerger, Rev. Mod. Phys. **80**, 885 (2008).

[28] B. A. Malomed and M. I. Weinstein, Phys. Lett. A **220**, 91 (1996).

[29] Y. Sivan, B. Ilan, and G. Fibich, Phys. Rev. E **78**, 046602 (2008).

[30] G. Gligorić, A. Maluckov, Lj. Hadžievski, and B. A. Malomed, Phys. Rev. A **81**, 013633 (2010).
[31] G. Gligorić, A. Maluckov, Lj. Hadžievski, and B. A. Malomed, Phys. Rev. A **79**, 053609 (2009); G. Gligorić, A. Maluckov, Lj. Hadžievski, and B. A. Malomed, *ibid.* A **78**, 063615 (2008).
[32] P. G. Kevrekidis, K. Ø. Rasmussen, and A. R. Bishop, Phys. Rev. E **61**, 2006 (2000).
[33] Yu. S. Kivshar and D. K. Campbell, Phys. Rev. E **48**, 3077 (1993).